Results in Chemistry 7 (2024) 101468

Contents lists available at ScienceDirect

Results in Chemistry

journal homepage: www.sciencedirect.com/journal/results-in-chemistry

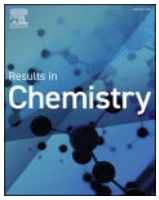

Biopreparation of cerium oxide nanoparticles using alginate: Characterization and estimation of antioxidant and its activity against breast cancer cell lines (MCF7)

Soudabe Mousaiyan, Javad Baharara, Ali Es-haghi *

Department of Biology, Mashhad Branch, Islamic Azad University, Mashhad, Iran

ARTICLE INFO

Keywords:
Breast cancer
Nanoparticle
Cytotoxicity
Cerium oxide
Antioxidant

ABSTRACT

Cerium is an important element whose various biomedical properties have been proven. The purpose of the current study was to fabricate cerium oxide nanoparticles (CeO-NPs) using alginate and to investigate their antioxidant properties and cytotoxicity against breast cancer cells and human skin fibroblasts. Cerium oxide nanoparticles were first synthesized using alginate, and their characteristics were then determined using XRD, FESEM, DLS, and FITR techniques. The antioxidant capacity of the prepared nanoparticles was measured using the DPPH biochemical method, and cytotoxicity was measured by the MTT method. Also, DAPI staining and annexin PI staining via flow cytometry were used to determine the type of cell death. Our findings indicated that the synthesized nanoparticles had IC_{50} values of 174, 32.5, and 16.07 μg/mL against the MCF-7 breast cancer cell line at 24, 48, and 72 h after treatment, respectively. Cell cycle assessment via flow cytometry revealed that the nanoparticles affected the ratio of the cells entering the apoptotic phase, supported by DAPI staining results showing the apoptotic activity of the synthesized nanoparticles. In conclusion, our results suggest that CeO-NPs can be considered as potential anti-cancer agents, and they are recommended to be further investigated in animal studies.

Introduction

Cancer is considered one of the serious problems in today's societies, caused by the complex interactions of genetic, epigenetic, and environmental factors [1–5]. The disease shows great diversity at the tissue, tumor, and cellular levels, explaining variable responses to existing treatments [6–8]. It is estimated that in 2030, cancer-related deaths will reach about 15 million [9]. Although chemotherapy can help treat cancer, the increase of multiple drug resistance (MDR) in cancer cells and the side effects of anticancer drugs are among the most important limitations of chemotherapy and major reasons for treatment failure [10,11]. Breast cancer is the most prevalent and most dreadful malignant disease among women worldwide, accounting for 23 % of all cancers among females [12–15].

Recently, green preparation of nanoparticles, as a simple, low-cost, and environmentally-friendly method and a replacement for physical and chemical methods, has gained special attention [16–20]. The biological effects of nanoparticles depend on their composition, concentration, size, physical and chemical properties, route and duration of exposure, as well as the type and growth stage of plant sources [21–24]. In green synthesis, plants, algae, microorganisms, and their components are used as regenerating agents to produce nanoparticles [25–28]. In today's cancer-targeted therapies, specifically designed nanoparticles are used to penetrate cancer cells and more effectively deliver anticancer drugs [29–31]. The distribution of nanoparticles is influenced by various parameters, including their size and concentration within cancer cells [32,33]. Cerium oxide nanoparticles are derived from oxidized forms of this rare element (i.e., cerium) and are capable of imitating the activity of superoxide dismutase and catalase owing to a shift in surface oxygen vacancies and valence arrangement. So, these nanoparticles can act as neutralizers of reactive oxygen species in many biological contexts [34,35]. New frontiers have been opened for nanoceria particles in biomedical research, including cancer therapy, diagnostic modalities, biosensors, etc. [36,37].

Alginate is a general name that refers to a set of natural non-branched polysaccharide polymers containing repeating units of β-D-mannuronic acid (M) and α-L-guluronic acid (G) attached via α1 → 4 glycosidic bonds [38]. Another feature that has greatly favored the use

* Corresponding author.
E-mail address: ashaghi@gmail.com (A. Es-haghi).

https://doi.org/10.1016/j.rechem.2024.101468
Received 15 January 2024; Accepted 27 March 2024
Available online 28 March 2024

of alginate as a bio-medical polymer, especially in recent years, is its capability as a carrier for various drugs and bio-molecules [39,40]. Despite many recent advances in the field of disease control and treatment, increased resistance of cancer cells to common therapeutics has become one of the global challenges in the field of human health, leading to undesirable responses to medications and failure of treatment measures [41]. Therefore, it is inevitable to expand the drugs isolated from natural products, which generally have fewer side effects and are capable of being modified to achieve more efficacy [42]. Natural compounds and their effective ingredients can be successfully used to treat various cancers in hospitals [43].

The present study aimed to biosynthesize cerium nanoparticles using alginate and then study their antioxidant and cytotoxic properties against a breast cancer cell line. The current study's novelty, or its unique contribution to the field, is twofold. Green Synthesis of CeO-NPs using alginate presents a new method for the synthesis of cerium oxide nanoparticles (CeO-NPs) using alginate. In this study, alginate is used as both a reducing and capping agent in the synthesis of CeO-NPs. This is a "green" or environmentally friendly method of synthesis, which is a significant advancement over traditional methods that often involve harsh chemicals and conditions. The CeO-NPs synthesized in this study also demonstrated significant cytotoxic effects against MCF-7 breast cancer cell lines. In the context of cancer treatment, a substance that can selectively kill cancer cells (like the MCF-7 breast cancer cells) without harming healthy cells is of great interest. This finding suggests that the CeO-NPs could potentially be used as a novel form of anticancer therapy. While other studies have also explored the green synthesis of CeO-NPs and their biomedical applications [44–46], the use of alginate as a reducing and capping agent and the demonstrated cytotoxic effects against MCF-7 breast cancer cell lines are unique aspects of this study. These findings not only contribute to the existing body of knowledge on CeO-NPs and their potential uses but also open up new avenues for future research in the field of anticancer therapies.

Materials and methods

1,1-Diphenyl-2-picrylhydrazyl (DPPH) was obtained from Sigma Chemicals Co. (St. Louis, MO, USA). Fetal bovine serum (FBS), trypsin, Dulbecco's Modified Eagle Medium (DMEM), antibiotic, 3,4,5-Dimethylthiazol-2-yl-2,5-diphenyltetrazolium bromide (MTT), 4′, 6-diamidino-2-phenylindole (DAPI), and sodium alginate were obtained from Sigma-Aldrich Company, Ltd. (Poole, United Kingdom). Annexin V–FITC apoptosis detection kit (ab14085) was purchased from Abcam, (Abcam Incorporated, Cambridge, MA). Other reagents were purchased from Merck (Germany). Human breast cancer cell line (MCF-7) and Human foreskin fibroblasts (HFF) were purchased from the Pasteur Institute of Iran (Tehran, Iran).

Synthesis of nanoparticles

To prepare CeO-NPs, 8.68 g of Ce $(NO_3)_3{\cdot}6H_2O$ salt was allowed to react with 200 mL of aqueous alginate sodium. Next, CeO–*O.* alginate was dried at 100 °C for 48 h, and finally, purified CeO-NPs were obtained by heating at 450 °C for 4 h and collecting brownish color pellets.

Characterization of CeO-NPs

Synthesized CeO-NPs were characterized using common techniques such as DLS, FESEM, XRD and FTIR [47]. The size of the NPs was examined by applying a Zetasizer apparatus (Nano-ZS, Malvern, UK). The morphology and the surface of CeO-NPs were seen by FESEM (JEOL, Japan). The crystal phase and purity of CeO-NPs were determined by applying Philips PW1800 X-ray diffractometer (XRD) (Almelo, Netherlands). The functional group on the surface of CeO-NP was determined by FTIR spectroscopy (Perkin Elmer, Waltham, MA, USA).

Evaluation of antioxidant activity by the DPPH method

The antioxidant capacity of the biosynthesized NPs was investigated by the DPPH radical scavenging method as reported by a previous study [48]. Different concentration concentrations of CeO-NPs were mixed in an equal volume of 0.1 mM of ethanol solution of DPPH. The mixture was incubated for 30 min at room temperature, and then the absorbance of the samples was read at 517 nm. Glutathione was used as a standard antioxidant compound. All tests were performed in triplicate.

Cytotoxicity assay

The cytotoxicity of CeO-NP was investigated against the MCF-7 breast cancer cell line. Also, the human foreskin fibroblast (HFF) cell line is used as a normal cell. Both cell lines were cultured in DMEM medium which was supplemented with 10 % fetal bovine serum (FBS) containing 100 UI/ml streptomycin and 100 μg/ml penicillin. The cells (5×10^3 cells/well) were seeded in 96-well plates and incubated at 37 °C in 5 % CO_2 for 24 h. After 24 h, cells were treated in triplicate with different concentrations of the CeO-NP and incubated for 24, 48, and 72 h. Finally, the cytotoxic activity was evaluated, using the MTT assay. Briefly, the supernatant was removed and washed three times with sterile 1x PBS. Then MTT solution (20 μL of a 5 mg/ml stock solution) was added and incubated at 37 °C for 4 h. At the end supernatant was discarded and produced formazan crystals were solved in 200 μL of DMSO. The absorbance was read at 570 nm using a plate reader spectrophotometer (Epoch, Biotek, Winooski, VT, United Kingdom).

DAPI staining

DAPI is a fluorescent dye that strongly binds to adenine–thymine-rich DNA sequences and is widely used in fluorescent microscopy. In this study, DAPI staining was used to visualize the nuclei of the cells treated with CeO-NPs and to check apoptosis, as well as chromatin condensation or fragmentation in these cells compared to the control group.

Apoptosis determination by flowcytometry assay

During the apoptosis, phosphatidylserine translocates from the inner to the outer layer of the plasma membrane. the use of annexin V together with propidium iodide provides the possibility of distinguishing between necrosis and apoptosis [49]. Annexin V-FITC Kit (ab14085) was used for this experiment. First, MCF7 cells were cultured in a 6-well plate and 24 h later, the cells were treated with the effective concentrations of CeO-NPs for 24 h. Then the cells were transferred into Eppendorf tubes, and centrifuged at 3000 rpm for five minutes by using a Bio-Rad tabletop centrifuge. After discarding the supernatant by aspiration, 500 μL of 1X Binding Buffer (provided by the kit) was added to each sample, and then 5 μL of annexin V and 5 μL of propidium iodide were added to each sample. The samples were taken for five minutes in a dark place and finally analyzed by flow cytometry instrument (FACSCalibur, Becton Dickinson, USA [50].

Statistical analysis

Statistical analysis was performed by SPSS Software (version 22) via one-way ANOVA and Duncan's multiple comparisons post-hoc test. p-value of < 0.05 was used as the cut-off for statistically significant observations. The results were represented as the mean ± standard deviation of three independent replications.

Results

Characterization

X-ray diffraction (XRD) is the best method used to analyze the crystal

structure of a material and nanomaterial. The reference code 01–081-0792 indicates a specific XRD pattern for Cerium Oxide, which can be used for comparison and identification purposes. It provided valuable insights into the synthesized CeO_2-NPs crystal structure (Fig. 1). It confirmed the prepared cerium oxide, with an empirical and chemical formula of CeO_2, belonged to the cubic crystal system with a space group of Fm-3 m (space group number 225). The XRD pattern displayed several diffraction peaks, each characterized by its Miller indices (*hkl*), interplanar spacing (d [A]), 2-theta angle (2Theta [deg]), and intensity (I [%]). Comparing the experimental values with the provided XRD pattern, we observed some similarities and differences. The first peak, indexed as (1 1 1), has an experimental 2-theta angle of 28.553(1)°, which is a little higher than the theoretical value of 28.542 degrees. The corresponding interplanar spacing is measured as 3.124 Å, which is near to the theoretical value of 3.125 Å. The experimental intensity is reported as 100 %, matching the theoretical value. For the second peak, indexed as (2 0 0), the experimental 2-theta angle is 33.093(3)°, moderately higher than the theoretical value of 33.075°. The experimental interplanar spacing is measured as 2.705 Å, which is near the theoretical value of 2.706 Å. However, the experimental intensity is reported as 32.55 %, higher than the theoretical value of 28.5 %. Similar comparisons can be made for the remaining peaks (Table 1), taking into account the experimental 2-theta values, interplanar spacings, and intensities. Overall, while there are slight variations between the experimental and theoretical values, the XRD pattern for Cerium Oxide (CeO2) provided a good match with the experimental data, confirming the crystal structure and aiding in the identification and characterization of the compound.

The XRD analysis has demonstrated, we successfully synthesized CeO_2-NPs using alginate as a stabilizing agent. The morphology of the synthesized nanoparticles was investigated using Field Emission Scanning Electron Microscopy (FESEM). The FESEM images (Fig. 2) revealed that the CeO_2-NPs exhibited a predominantly spherical and semi-spherical shape. However, it was observed that the nanoparticles were highly agglomerated, forming clusters or aggregates. Fig. 3, which depicts the FESEM image, provides visual evidence of the agglomeration phenomenon. The agglomerates appear as larger structures composed of multiple nanoparticles clustered together.

In addition to the FESEM analysis, we also determined the size distribution of the synthesized CeO2-NPs using the dynamic light scattering (DLS) technique. Fig. 3 displays the results obtained from the DLS analysis, which revealed a narrow size distribution of the nanoparticles. The average diameter of the CeO2-NPs was measured to be 83 nm, indicating that the nanoparticles were predominantly in the nanoscale range. The polydispersity index (PDI) value of 0.192 suggests a relatively uniform size distribution, indicating minimal variation in particle sizes. To improve the dispersity of the CeO_2-NPs, we employed a probe sonicator, which is a common technique used to disperse and break up agglomerates in liquid suspensions. The DLS analysis showed that the use of the probe sonicator resulted in good dispersity of the nanoparticles in the liquid phase. This suggests that the agglomeration observed in the FESEM images, which were obtained from the solid phase, was reduced when the nanoparticles were dispersed in a liquid medium. The comparison between the FESEM images and the DLS analysis highlights the difference in the agglomeration behavior of the CeO_2-NPs between the solid and liquid phases. The FESEM images showed that the nanoparticles were highly agglomerated in the solid phase, forming clusters or aggregates. However, the DLS analysis indicated that the nanoparticles had good dispersity in the liquid phase, with a narrow size distribution. This difference can be attributed to the influence of the surrounding medium. In the solid phase, the nanoparticles may experience stronger attractive forces and limited mobility, leading to increased agglomeration. However, when dispersed in a liquid medium, the nanoparticles experience reduced interparticle interactions and increased Brownian motion, resulting in improved dispersity and reduced agglomeration. The combination of FESEM and DLS analyses provided a comprehensive understanding of the morphology and size distribution of the CeO_2-NPs. While the FESEM images revealed agglomeration in the solid phase, the DLS analysis demonstrated good dispersity in the liquid phase after using a probe sonicator. This information is crucial for optimizing the synthesis process and understanding the behavior of the CeO_2-NPs in different environments.

The FTIR (Fourier Transform Infrared) spectrum of the CeO_2-NPs provided valuable information about the chemical composition and

Table 1
The theoretical values related to crystal structure of the reference code's XRD pattern (01–081-0792).

No.	h	k	l	d [A]	2Theta[deg]	I [%]
1	1	1	1	3	28.542	100
2	2	0	0	3	33.075	28.5
3	2	2	0	2	47.475	45.8
4	3	1	1	2	56.332	36.1
5	2	2	2	2	59.078	7.1
6	4	0	0	1	69.401	5.8
7	3	3	1	1	76.685	12.5
8	4	2	0	1	79.06	8.7
9	4	2	2	1	88.41	10.3

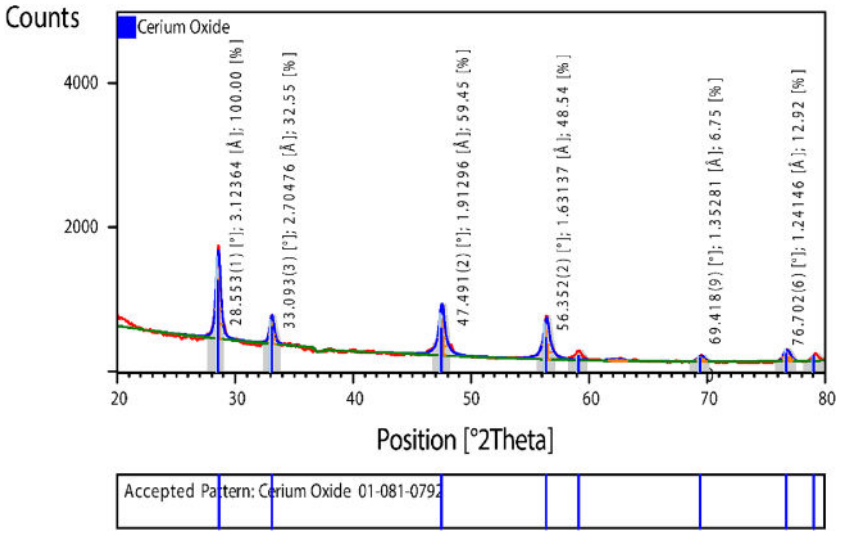

Fig. 1. XRD spectrum analysis of cerium oxide nanoparticles synthesized by alginate.

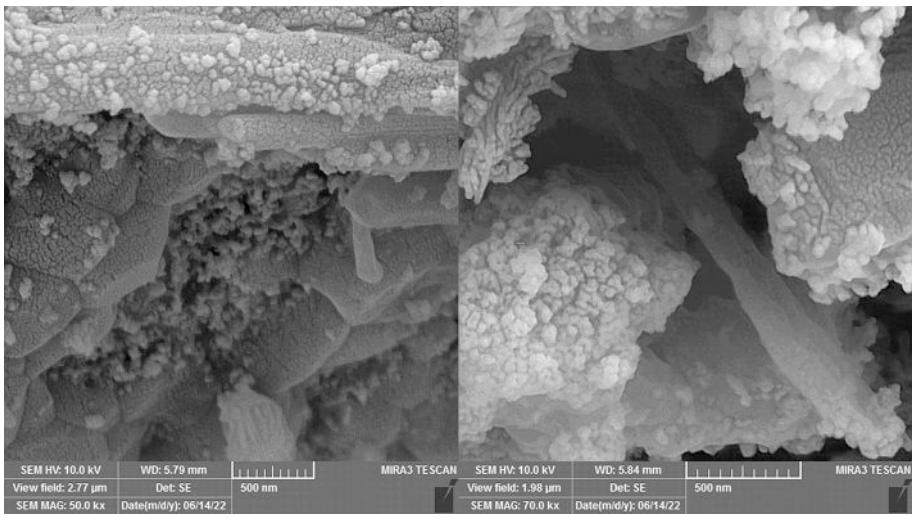

Fig. 2. FESEM imaging of cerium oxide nanoparticle synthesized by alginate.

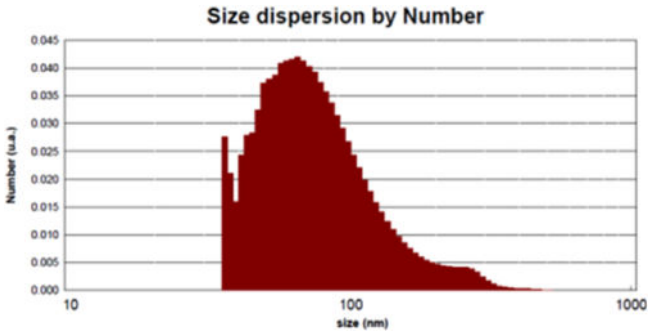

Fig. 3. DLS method, Dispersion of cerium nanoparticles synthesized by alginate.

surface characteristics of the nanoparticles (Fig. 4). One of the observed bands at 425 cm^{-1} corresponds to a characteristic vibration related to the cubic crystalline form of rare earth oxides, specifically CeO_2-NPs. This band confirmed the presence of cerium oxide bonds in the nanoparticles. The band observed at 1446 cm^{-1} represented the N = O stretching vibration, which suggested the presence of a small amount of nitrate in the prepared sample. The band that appeared at 2969 cm^{-1} is assigned to the C-H stretching vibration of the residual biopolymer. This band suggested the presence of organic materials, possibly residual alginate, on the surface of the CeO_2-NPs. Lastly, the band at 3310 cm^{-1} corresponded to the stretching vibration of H-bonded water molecules. This peak indicated the presence of absorbed water molecules that were physically connected to the surface of the CeO_2-NPs [44,51,52]. In summary, The FTIR bands in the CeO_2-NPs spectrum suggested the presence of cerium oxide bonds, residual organic materials, and absorbed water molecules. This information provides insights into the chemical composition and surface characteristics of the CeO_2-NPs, which is valuable for understanding their properties and potential applications.

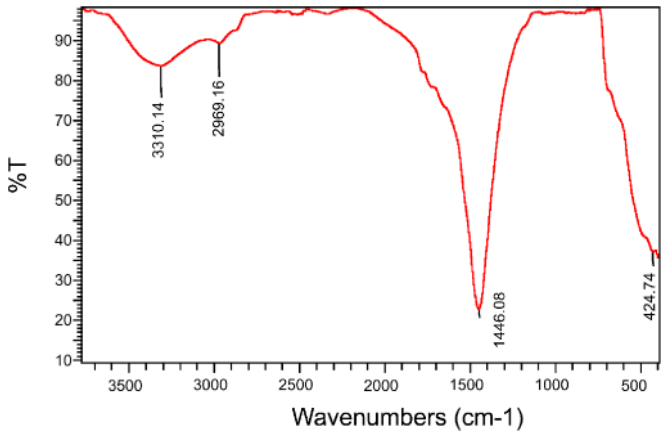

Fig. 4. FTIR spectra of cerium oxide nanoparticle synthesized by alginate.

Free radical scavenging capacity of CeO-NPs

2,2-diphenyl-1-picrylhydrazyl (DPPH), is a radical scavenger because it can accept electrons from reactive radicals. The mechanism of DPPH free radical scavenging may be very complex because the DPPH molecules not only can react with electrophile reagents but also can react with hydroxyl radicals. The antioxidant capacity of compounds was recorded based on photobleaching of DPPH at 517 nm. The antioxidant capacity of CeO-NPs was determined by the DPPH free radical scavenging assay (Fig. 5). The results indicated that green synthesized NPs significantly inhibited DPPH free radicals in a dose-dependent manner. The IC50 of CeO-NPs (i.e., the concentration inhibiting 50 % of DPPH free radicals) was obtained at 31.25 µg/mL. Glutathione was used as a positive control in this experiment.

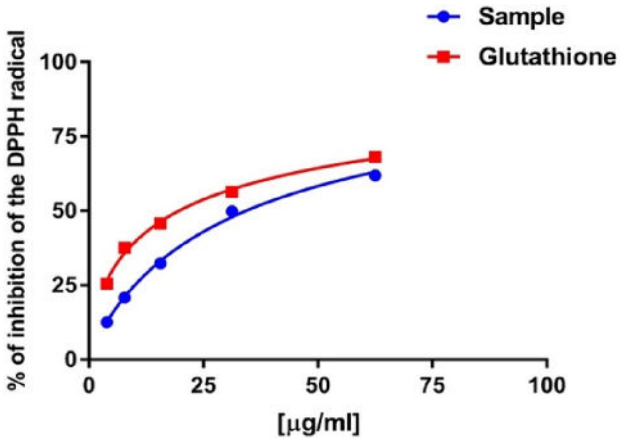

Fig. 5. DPPH scavenging assay of CeO-NPs synthesized by alginate. Glutathione was used as a positive control. The experiment was conducted in triplicate.

Evaluation of cytotoxicity

The cytotoxicity of the CeO-NPs synthesized was performed against a breast cancer cell line (MCF-7) and a normal cell line (HFF). First cells were treated with different concentrations of CeO-NPs ranging from 0 to 300 μg/mL. During the period of 24, 48, and 72 h the viability of cells was checked using MTT assay. According to the results present in Fig. 6, the viability of MCF-7 cells was significantly inhibited in the presence of CeO-NP in a dose-dependent manner, while HFF cells were less prone to the presence of CeO-NPs as compared to the cancerous cells. Evaluation of the viability of MCF-7 cells demonstrated IC_{50} values of 174, 32.5, and 16.07 μg/mL at 24, 48, and 72 h after treatment, respectively (Fig. 6).

Morphological examination by DAPI fluorescent staining

The results of the cell toxicity assay represented that CeO-NPs effectively inhibited the growth of cancer cells, prompting further evaluations of possible toxicity mechanisms against the MCF-7 cell line. Morphological changes in MCF-7 cells (as shown by DAPI staining) treated with different concentrations of CeO-NPs including 0, 87, 174, and 348 μg/ml have been shown in Fig. 7 prominent morphological changes, including plasma membrane blebbing, cell shrinkage, and destruction of cells were observed in cancerous cells exposed to CeO-NPs for 24 h, suggesting apoptotic cell death. The nuclei of the cells were examined by a fluorescent microscope. In the control group (i.e., no treatment), the nuclei of the cells were observed to be uniform and intact. The results showed that increasing concentrations of CeO-NPs led the nuclei of the cells to become fragmented and decomposed.

Cell death evaluation by the annexin V-FITC assay

Flow cytometry assay of the MCF-7 cancer cells treated with 87, 174, and 348 μg/mL of CeO-NPs revealed that primary apoptosis, secondary apoptosis, and necrosis were observed in 2.9 %, 15.6 %, and 2.2 % of the cells exposed to the 87 μg/mL concentration and 3.5 %, 32.2 %, and 2.5 % of the cells treated with the 174 μg/mL concentration, respectively. Finally, in the cells treated with the 348 μg/mL concentration, more than half of the cells underwent secondary apoptosis while necrosis was noticed in > 33 % of the cells (Fig. 8).

Discussion

Today, the growing resistance of cancers to ordinary treatments has become a serious problem, and existing treatments have failed to meet the therapeutic requirements demanded by most types of cancers [53–55]. So, the use of new technologies for preventing and treating cancer can be a solution [56–58]. Resistance of cancer cells to chemical drugs and chemotherapeutics is a main cause of treatment failure, highlighting requirements for extensive research and development on more efficient drugs with fewer side effects [59,60]. Among various metal oxide nanoparticles, ceria nanoparticles have attracted considerable attention and interest due to their unique properties such as radical scavenging activity and a wide range of other biological effects, offering promising medical and biomedical applications for these nanoparticles [61,62]. In the present study, CeO-NPs were fabricated using alginate and characterized by multiple techniques, including DLS, XRD, and FESEM, which confirmed the nano-scale of the NPs synthesized. The MTT cytotoxicity assay showed that CeO-NPs were efficient in preventing the growth of MCF-7 breast cancer cells compared with normal cells, which was supported by morphological changes observed in these cells. A recent study performed by Nourmohammadi *et al.* demonstrated the cell toxicity effects of CeO-NPs against mouse fibrosarcoma cell line [63]. Various similar studies have shown the anticancer possibility of CuO-NPs against different cancer cell lines [64]. In another research, Hijaz *et al.* investigated the effects of cerium nanoparticles on the A2780 ovarian cancer cell line, reporting concentration-dependent growth inhibitory effects [65]. Also, cytotoxicity and growth inhibitory effects were observed against other ovarian cancer cell lines (SKOV3, OVCAR 3, and C200) as well.

Cerium nanoparticles are metal-based compounds reported to have toxicity against a variety of cancer cells by inhibiting their growth and invasion, sensitizing them to radiation and chemotherapy, protecting these cells against reactive oxygen species (ROS), and inducing apoptosis in cancerous cells [66–69]. When assessing how different synthesis techniques affect the effectiveness of CeO-NPs in cellular inhibition or apoptosis, it's crucial to distinguish between the outcomes produced by green synthesis and chemical synthesis methods. Green synthesis, which utilizes natural compounds as reducing and capping agents, often results in nanoparticles with diverse size distributions and morphologies [70]. These variations can significantly impact their surface area and reactivity, influencing their interactions with cells and their ability to inhibit or induce cell death. In contrast, chemical synthesis may introduce more defects or impurities, potentially altering the cytotoxicity of the nanoparticles. Furthermore, the surface chemistry of green-synthesized nanoparticles, influenced by biological molecules, can enhance biocompatibility and enable targeted delivery to cells, thus increasing their therapeutic potential [71]. Additionally, the antioxidant and antimicrobial properties displayed by green-synthesized nanoparticles are crucial for biomedical applications, particularly in cancer therapy. Finally, it's important to consider the environmental impact of nanoparticle production. Green synthesis offers a more sustainable and eco-friendly approach, underscoring its significance beyond mere procedural considerations [72]. Ultimately, the choice of synthesis method plays a pivotal role in shaping the therapeutic effectiveness and range of applications of CeO-NPs [73,74]. In a study, Nasiri *et al.* investigated the cytotoxicity of CeO-NPs at different concentrations and times against HT29 clone cancer cells and showed that the nanoparticles offered the most potent toxicity at concentrations between 12.5 and 100 mg/mL in a time- and concentration-dependent manner, arguing that at longer exposure times, the nanoparticles had more opportunity to enter the cells and exert their toxicity effects (e.g., via inducing oxidative stress and producing toxic oxygen radicals). Sandeep *et al.* (2014) investigated

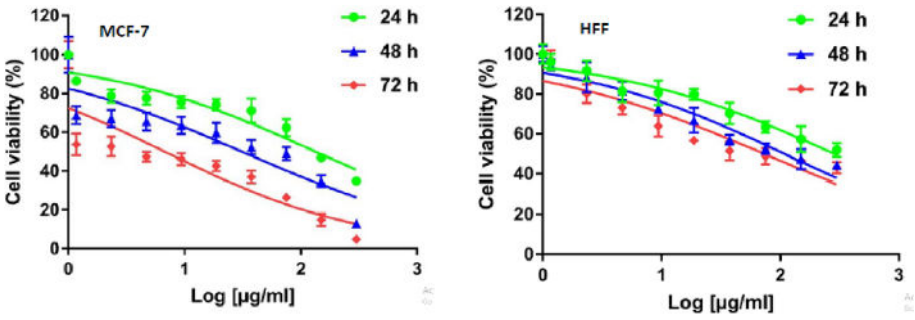

Fig. 6. Cell toxicity of ceo-nps at different concentrations against the breast cancer cell MCF-7 and HFF cell lines. Results are presented as the mean ± SD (n = 3).

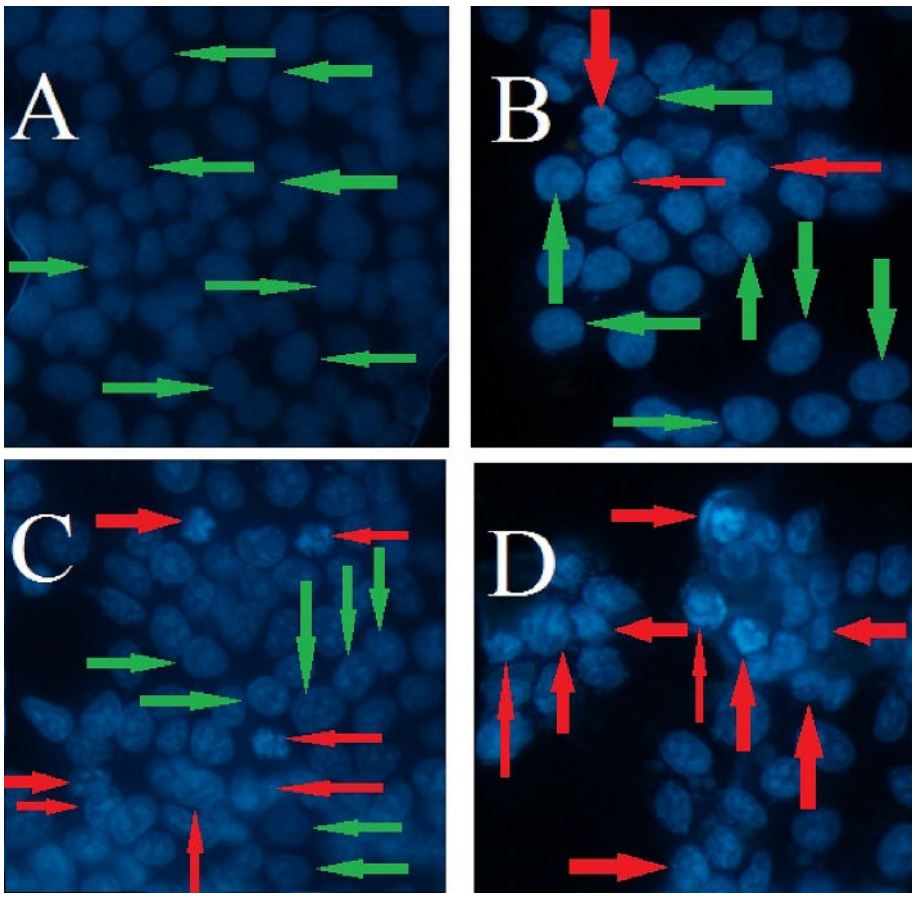

Fig. 7. Stages of cancer cell death. A) Control group: the nuclei of the cells are intact and unchanged. B) Cells treated with the 87 μg/mL concentration: the arrowheads indicate MCF-7 cancer cells, showing no specific morphological changes. C) Cell treated with the 174 μg/mL concentration: arrowheads indicate shrunken small (shiny) and apoptotic MCF-7 cancer cells, reflecting chromatin fragmentation. D) Cells treated with the 348 μg/mL concentration: the nucleus of most cancer cells showed fragmentation, indicating cell death.

the effects of cerium nanoparticles on lung cancer cells (A549) and showed that these nanoparticles exerted significant toxicity and morphological changes in these cells. The HCT116 colorectal cancer cells exposed to different concentrations (5, 10, 20, 40, 60, 80, and 100 μg/mL) of cerium nanoparticles underwent apoptotic cell death (confirmed via Annexin V test and DAPI staining) with an IC50 equal to 50.48 μg/mL, revealing more toxicity compared to most available anticancer drugs [75]. In 2022, Javid *et al.* investigated the toxicity of cerium nanoparticles against esophageal cancer cells (the YM1 and CSC-LC cell lines), reporting that cerium nanoparticles triggered cell death in a dose- and time-dependent manner in cancerous cells while they had no adverse effects on normal cells, suggesting the potential role of CeO-NPs as an effective anticancer treatment. In general, further studies, including animal and clinical studies, are required to elucidate the antitumor mechanisms employed by CeO-NPs in various cancers.

The study presented herein, while comprehensive, acknowledges certain limitations that must be considered. Firstly, the synthesis and characterization of cerium oxide nanoparticles using alginate were confined to specific analytical techniques, which may not encompass the full spectrum of nanoparticle behavior. Secondly, the cytotoxicity assessments were limited to in vitro conditions, which do not fully replicate the complex in vivo environment. The observed anticancer effects against MCF-7 breast cancer cell lines, while promising, require validation through in vivo studies to confirm efficacy and safety. Additionally, the antioxidant properties were measured using a single method, and further studies employing a variety of assays are recommended to provide a more comprehensive understanding of the nanoparticles' capabilities. Lastly, the potential impact of CeO-NPs on the environment and long-term biocompatibility remains to be thoroughly investigated. These limitations highlight the need for further research to explore the full potential and implications of CeO-NPs in biomedical applications.

Conclusion

This study presents an eco-friendly approach to synthesizing cerium oxide nanoparticles (CeO-NPs) using alginate, a natural polymer. The synthesized CeO-NPs were characterized by various techniques, confirming their nanoscale size (83 nm) and spherical morphology. The antioxidant activity was demonstrated with an IC50 of 31.25 μg/mL in the DPPH assay, indicating a potent ability to neutralize free radicals. The cytotoxic potential of CeO-NPs was evaluated against MCF-7 breast cancer cells, revealing significant inhibitory effects in a dose- and time-dependent manner, with IC50 values of 174, 32.5, and 16.07 μg/mL at 24, 48, and 72 h' post-treatment, respectively. Additionally, the nanoparticles induced apoptosis in cancer cells, as evidenced by DAPI staining and flow cytometry. These findings underscore the promise of CeO-NPs as chemotherapeutic agents, with their ability to selectively target cancer cells while exhibiting minimal toxicity towards normal cells. While our findings are promising, further research is necessary to fully understand the mechanisms behind the anticancer activity of CeO-NPs. Future studies should focus on testing the CeO-NPs in animal models to evaluate their efficacy and safety profile in a living organism, elucidating the precise biochemical pathways through which CeO-NPs exert their cytotoxic effects on cancer cells. developing targeted delivery systems for CeO-NPs to minimize potential side effects and

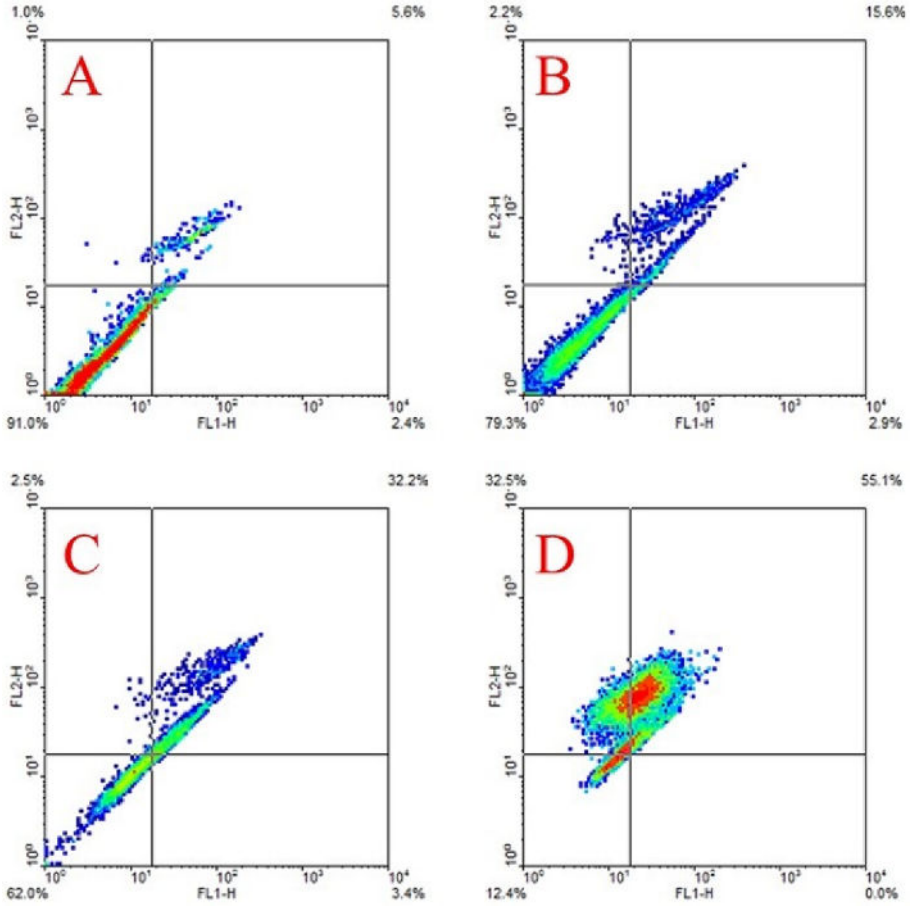

Fig. 8. Death rate in MCF-7 cancer cells treated with cerium nanoparticles: (A) The control group (non-treated MCF-7 cancer cells). More than 91 % of the cells were alive (i.e., apoptosis rate = 9 %, probably caused by the stress of displacement). MCF-7 cancer cells treated with 77 μg/mL (B) (viable cells > 75 %, apoptosis rate = 3 %), 174 μg/mL (C) (viable cells = 62 %, apoptosis rate < 4 %), and 348 μg/mL (D) (viable cells < 13 %, apoptosis rate > 5 %) concentrations.

enhance therapeutic outcomes, and finally investigating the synergistic effects of CeO-NPs when combined with conventional chemotherapy or other nanomedicine-based therapies. By addressing these areas, we can pave the way for CeO-NPs to become a viable option in the arsenal of anticancer treatments. The potential of CeO-NPs as chemotherapeutic agents warrants further exploration, with the ultimate goal of translating these findings into clinical applications.

Funding

None.

Declarations.

Ethical Approval.

Not applicable.

Availability of data and materials.

The authors declare that the data supporting the findings of this study are available within the paper.

CRediT authorship contribution statement

Sodabeh Mousayian: Software, Methodology, Investigation, Formal analysis, Data curation, Conceptualization. **Javad Baharara:** Validation, Software, Formal analysis. **Ali Es-haghi:** Writing – review & editing, Writing – original draft, Supervision, Project administration, Methodology, Formal analysis, Conceptualization.

Declaration of competing interest

The authors declare that they have no known competing financial interests or personal relationships that could have appeared to influence the work reported in this paper.

Acknowledgement

The authors appreciatively acknowledge for support and assistance provided by the Mashhad branch of Islamic Azad University.

References

[1] A. Mbemi, S. Khanna, S. Njiki, C.G. Yedjou, P.B. Tchounwou, Impact of gene–environment interactions on cancer development, Int. J. Environ. Res. Public Health 17 (21) (2020) 8089.
[2] V. Mohammadzadeh, N. Rahiman, H. Cabral, S. Quader, M.R. Zirak, M.E.T. Yazdi, et al., Poly-γ-glutamic acid nanoparticles as adjuvant and antigen carrier system for cancer vaccination, J. Control. Release 362 (2023) 278–296.
[3] L.U. Sarder, S. Ahmad, Emerging role of biosimilars: focus on trastuzumab and metastatic human epidermal growth factor receptor 2-positive breast cancer, Results Chem. 6 (2023) 101055.
[4] A.J. Hadi, U.M. Nayef, M.S. Jabir, F.-A.-H. Mutlak, Synthesis of vanadium pentoxide nanoparticles via laser ablation for biomedical applications, Int. J. Mod Phys B (2023) 2450230.
[5] A.J. Hadi, U.M. Nayef, M.S. Jabir, F.A. Mutlak, Titanium dioxide nanoparticles prepared via laser ablation: evaluation of their antibacterial and anticancer activity, Surface Rev. Lett. (SRL). 30 (10) (2023) 1–10.
[6] I. Dagogo-Jack, A.T. Shaw, Tumour heterogeneity and resistance to cancer therapies, Nat. Rev. Clin. Oncol. 15 (2) (2018) 81–94.
[7] A. Es-haghi, M.E. Taghavizadeh Yazdi, M. Sharifalhoseini, M. Baghani, E. Yousefi, A. Rahdar, et al., Application of response Surface methodology for optimizing the

therapeutic activity of ZnO Nanoparticles Biosynthesized from Aspergillus niger, Biomimetics. 6 (2) (2021) 34.
[8] M.E. Taghavizadeh Yazdi, M. Qayoomian, S. Beigoli, M.H. Boskabady, Recent advances in Nanoparticles applications in respiratory Disorders, a review, Front. Pharmacol. 14 (2023) 1059343.
[9] C. Mattiuzzi, G. Lippi, Current cancer epidemiology, J. Epidemiol. Global Health. 9 (4) (2019) 217.
[10] R. Pokhriyal, R. Hariprasad, L. Kumar, G. Hariprasad, Chemotherapy resistance in advanced ovarian cancer patients, Biomarkers in Cancer. 11 (2019), 1179299X19860815.
[11] N.S. Fateme Momen Eslamieh-ei, S.A.P. Tousi, S. Basharkhah, J. Mottaghipisheh, A. Es-haghi, M.E.T. Yazdi, M. Iriti, Synthesis and its characterisation of selenium/silver/chitosan and cellular toxicity against liver carcinoma cells studies, Nat. Prod. Res. (2023).
[12] Mandal V, Sharma N, Katiyar P, Agrawal M, Maurya AK. A REVIEW ARTICLE ON BREAST CANCER.
[13] T. Yin, R. Wang, S. Yang, Anti-breast cancer activity of co (II) complex by inhibiting cell viability and stimulating cell apoptosis, J. Clust. Sci. 1–8 (2022).
[14] E. Rahimi, F. Asefi, A. Afzalinia, S. Khezri, H. Zare-Zardini, A. Ghorani-Azam, et al., Chitosan coated copper/silver oxide nanoparticles as carriers of breast anticancer drug: cyclin D1/P53 expressions and cytotoxicity studies, Inorg. Chem. Commun. 111581 (2023).
[15] M.E.T. Yazdi, M.S. Amiri, S. Akbari, M. Sharifalhoseini, F. Nourbakhsh, M. Mashreghi, et al., Green synthesis of silver nanoparticles using helichrysum graveolens for biomedical applications and wastewater treatment, BioNanoScience. 10 (4) (2020) 1121–1127.
[16] S.D. Jo, S.H. Ku, Y.-Y. Won, S.H. Kim, I.C. Kwon, Targeted nanotheranostics for future personalized medicine: recent progress in cancer therapy, Theranostics. 6 (9) (2016) 1362.
[17] S.M. Mousavi-Kouhi, A. Beyk-Khormizi, V. Mohammadzadeh, M. Ashna, A. Es-haghi, M. Mashreghi, et al., Biological synthesis and characterization of gold nanoparticles using Verbascum speciosum schrad. and cytotoxicity properties toward HepG2 cancer cell line, Res. Chem. Intermed. 48 (1) (2022) 167–178.
[18] T. Saranya, S. Ramya, K. Kavithaa, M. Paulpandi, Y.-P. Cheon, S. Harysh Winster, et al., Green synthesis of selenium nanoparticles using solanum nigrum fruit extract and its anti-cancer efficacy against triple negative breast cancer, J. Clust. Sci. 1–11 (2022).
[19] R.A. Mohammed, F.A. Mutlak, G.M. Saleh, Structural and optical properties of green spinach extract leaf (spincia olercea) prepared with silver nanoparticles as antibacterial by effect of pulsed laser, J. Opt. 1–9 (2021).
[20] Aswad MA, Mutlak FA, Jabir MS, Abdulridha SK, Ahmed AF, Nayef UM, editors. Laser assisted hydrothermal synthesis of magnetic ferrite nanoparticles for biomedical applications. Journal of Physics: Conference Series; 2021: IOP Publishing.
[21] J.K. Patra, G. Das, L.F. Fraceto, E.V.R. Campos, M.P. Rodriguez-Torres, L.S. Acosta-Torres, et al., Nano based drug delivery systems: recent developments and future prospects, J. Nanobiotechnol. 16 (1) (2018) 1–33.
[22] M.S. Amiri, M.E.T. Yazdi, M. Rahnama, Medicinal plants and phytotherapy in Iran: glorious history, current status and future prospects, Plant Science Today. 8 (1) (2021) 95–111.
[23] M.M.N. Halimi Khalil Abad, M.E.T. Yazdi, Biosynthesis of ZnO.Ag2O3 using aqueous extract of Haplophyllum obtusifolium: Characterization and cell toxicity activity against liver carcinoma cells. micro, Nano Lett. (2023) 18.
[24] A.J. Hadi, U.M. Nayef, F.-A.-H. Mutlak, M.S. Jabir, Laser-ablated zinc oxide nanoparticles and evaluation of their antibacterial and anticancer activity against an ovarian cancer cell line: in vitro study, Plasmonics 18 (6) (2023) 2091–2101.
[25] C. Pandit, A. Roy, S. Ghotekar, A. Khusro, M.N. Islam, T.B. Emran, et al., Biological agents for synthesis of nanoparticles and their applications, Journal of King Saud University-Science. 34 (3) (2022) 101869.
[26] K. Shakerimanesh, F. Bayat, A. Shahrokhi, A. Baradaran, E. Yousefi, M. Mashreghi, et al., Biomimetic synthesis and characterisation of homogenouse gold nanoparticles and estimation of its cytotoxity against breast cancer cell line, Mater. Technol. 1–8 (2022).
[27] H. Zarharan, M. Bagherian, A.S. Rokhi, R.R. Bajgiran, E. Yousefi, P. Heravian, et al., The anti-angiogenesis and antioxidant activity of chitosan-mediated synthesized selenium-gold nanostructure, Arab. J. Chem. 16 (7) (2023) 104806.
[28] M.S. Bagherian, P. Zargham, H. Zarharan, M. Bakhtiari, N. Mortezaee Ghariyeh Ali, E. Yousefi, et al., Antimicrobial and antibiofilm properties of selenium-chitosan-loaded salicylic acid nanoparticles for the removal of emerging contaminants from bacterial pathogens, World J. Microbiol. Biotechnol. 40(3):86 (2024).
[29] Z. Cheng, M. Li, R. Dey, Y. Chen, Nanomaterials for cancer therapy: current progress and perspectives, J. Hematol. Oncol. 14 (1) (2021) 1–27.
[30] M.E. Taghavizadeh Yazdi, M. Darroudi, M.S. Amiri, H. Zarrinfar, H.A. Hosseini, M. Mashreghi, et al., Antimycobacterial, anticancer, antioxidant and photocatalytic activity of biosynthesized silver nanoparticles using Berberis integerrima, Iranian Journal of Science and Technology, Transactions a: Science. 46 (1) (2022) 1–11.
[31] S. Abdulzehra, D. Jafari-Gharabaghlou, N. Zarghami, Targeted delivery of oxaliplatin via folate-decorated niosomal nanoparticles potentiates resistance reversion of colon cancer cells, Heliyon. (2023).
[32] A.A. Al-Khedhairy, R. Wahab, Size-dependent cytotoxic and Molecular study of the use of gold Nanoparticles against liver cancer cells, Appl. Sci. 12 (2) (2022) 901.
[33] F. Mobaraki, M. Momeni, M.E.T. Yazdi, Z. Meshkat, M.S. Toosi, S.M. Hosseini, Plant-derived synthesis and characterization of gold nanoparticles: investigation of its antioxidant and anticancer activity against human testicular embryonic carcinoma stem cells, Process Biochem. 111 (2021) 167–177.
[34] S. Chen, Y. Hou, G. Cheng, C. Zhang, S. Wang, J. Zhang, Cerium oxide nanoparticles protect endothelial cells from apoptosis induced by oxidative stress, Biol. Trace Elem. Res. 154 (1) (2013) 156–166.
[35] A. Ghorani-Azam, J. Mottaghipisheh, M.S. Amiri, M. Mashreghi, A. Hashemzadeh, A. Haddad-Mashadrizeh, et al., Resveratrol-mediated gold-nanoceria synthesis as green nanomedicine for phytotherapy of Hepatocellular Carcinoma, Frontiers in Bioscience-Landmark. 27 (8) (2022) 227.
[36] H. Liying, S. Yumin, J. Lanhong, S. Shikao, Recent advances of cerium oxide nanoparticles in synthesis, luminescence and biomedical studies: a review, J. Rare Earths 33 (8) (2015) 791–799.
[37] M. Ashna, A. Es-Haghi, M. Karimi Noghondar, D. Al Amara, M.E.T. Yazdi, Greener synthesis of cerium oxide nanoemulsion using pollen grains of Brassica napus and evaluation of its antitumour and cytotoxicity properties, Mater. Technol. 37 (8) (2022) 525–532.
[38] I. Vroman, L. Tighzert, Biodegradable polymers, Materials. 2 (2) (2009) 307–344.
[39] S. Jana, K. Kumar Sen, A. Gandhi, Alginate based nanocarriers for drug delivery applications, Curr. Pharm. Des. 22 (22) (2016) 3399–3410.
[40] Z. Feyissa, G.D. Edossa, N.K. Gupta, D. Negera, Development of double crosslinked sodium alginate/chitosan based hydrogels for controlled release of metronidazole and its antibacterial activity, Heliyon. 9 (9) (2023).
[41] X. Wang, H. Zhang, X. Chen, Drug resistance and combating drug resistance in cancer, Cancer Drug Resistance. 2 (2) (2019) 141.
[42] A.G. Atanasov, S.B. Zotchev, V.M. Dirsch, C.T. Supuran, Natural products in drug discovery: advances and opportunities, Nat. Rev. Drug Discov. 20 (3) (2021) 200–216.
[43] Kashyap D, Tuli HS, Yerer MB, Sharma A, Sak K, Srivastava S, et al., editors. Natural product-based nanoformulations for cancer therapy: Opportunities and challenges. Seminars in cancer biology; 2021: Elsevier.
[44] F. Asgharzadeh, A. Hashemzadeh, F. Rahmani, A. Yaghoubi, S.E. Nazari, A. Avan, et al., Cerium oxide nanoparticles acts as a novel therapeutic agent for ulcerative colitis through anti-oxidative mechanism, Life Sci. 278 (2021) 119500.
[45] M.A. Khan, M.A.R. Siddique, M. Sajid, S. Karim, M.U. Ali, R. Abid, et al., A Comparative study of green and chemical cerium oxide Nanoparticles (CeO2-NPs): from synthesis, Characterization, and electrochemical analysis to Multifaceted biomedical applications, BioNanoScience. 13 (2) (2023) 667–685.
[46] N. Yadav, Cerium oxide nanostructures: properties, biomedical applications and surface coatings. 3, Biotech (2022;12(5):121.).
[47] B. Kumar, K. Smita, L. Cumbal, Debut AJSjobs, Green Synthesis of Silver Nanoparticles Using Andean Blackberry Fruit Extract. 24 (1) (2017) 45–50.
[48] M.P. Kumar, D. Ayodhya, Novel copper (II) binary complexes with N, O-donor isoxazole schiff base ligands: synthesis, characterization, DPPH scavenging, antimicrobial, and DNA binding and cleavage studies, Results in Chemistry. 5 (2023) 100845.
[49] J.P. Aubry, A. Blaecke, S. Lecoanet-Henchoz, P. Jeannin, N. Herbault, G. Caron, et al., Annexin V used for measuring apoptosis in the early events of cellular cytotoxicity, Cytometry: the Journal of the International Society for Analytical Cytology. 37 (3) (1999) 197–204.
[50] E. Miller, Apoptosis measurement by annexin v staining, Springer, Cancer cell culture, 2004, pp. 191–202.
[51] L. Hasanzadeh, R. Kazemi Oskuee, K. Sadri, E. Nourmohammadi, M. Mohajeri, Z. Mardani, et al., Green synthesis of labeled CeO2 nanoparticles with 99mTc and its biodistribution evaluation in mice, Life Sci. 212 (2018) 233–240.
[52] E. Nourmohammadi, R. Kazemi Oskuee, L. Hasanzadeh, M. Mohajeri, A. Hashemzadeh, M. Rezayi, et al., Cytotoxic activity of greener synthesis of cerium oxide nanoparticles using carrageenan towards a WEHI 164 cancer cell line, Ceram. Int. 44 (16) (2018) 19570–19575.
[53] Taghavizadeh Yazdi ME, Amiri MS, Darroudi M. Biopolymers in the Synthesis of Different Nanostructuresavizadeh 2020.
[54] M. Nadaf, M.S. Amiri, M.R. Joharchi, R. Omidipour, M. Moazezi, B. Mohaddesi, et al., Ethnobotanical diversity of trees and shrubs of Iran: a comprehensive review, International Journal of Plant Biology. 14 (1) (2023) 120–146.
[55] R. Ahmadi, A. Es-haghi, H. Zare-Zardini, M.E. Taghavizadeh Yazdi, Nickel oxide nanoparticles synthesized by rose hip extract exert cytotoxicity against the HT-29 colon cancer cell line through the caspase-3/caspase-9/Bax pathway, Emergent Materials. (2023) 1–12.
[56] F. Mobaraki, M. Momeni, M. Jahromi, F.M. Kasmaie, M. Barghbani, M.E.T. Yazdi, et al., Apoptotic, antioxidant and cytotoxic properties of synthesized AgNPs using green tea against human testicular embryonic cancer stem cells, Process Biochem. (2022).
[57] M. Darroudi, M.E.T. Yazdi, M.S. Amiri, Plant-mediated Biosynthesis of Nanoparticles. 21st century nanoscience–a handbook, CRC Press (2020) 1–18.
[58] Z. Shamasi, A. Es-haghi, M.E. Taghavizadeh Yazdi, M.S. Amiri, M. Homayouni-Tabrizi, Role of Rubia tinctorum in the synthesis of zinc oxide nanoparticles and apoptosis induction in breast cancer cell line, Nanomedicine Journal. 8 (1) (2021) 65–72.
[59] K. Bukowski, M. Kciuk, R. Kontek, Mechanisms of multidrug resistance in cancer chemotherapy, Int. J. Mol. Sci. 21 (9) (2020) 3233.
[60] S.M. Mousavi-Kouhi, A. Beyk-Khormizi, M.S. Amiri, M. Mashreghi, M.E.T. Yazdi, Silver-zinc oxide nanocomposite: from synthesis to antimicrobial and anticancer properties, Ceram. Int. 47 (15) (2021) 21490–21497.
[61] M. Nadeem, R. Khan, K. Afridi, A. Nadhman, S. Ullah, S. Faisal, et al., Green synthesis of cerium oxide nanoparticles (CeO2 NPs) and their antimicrobial applications: a review, Int. J. Nanomed. 15 (2020) 5951.
[62] F. Javadi, M.E.T. Yazdi, M. Baghani, A. Es-haghi, Biosynthesis, characterization of cerium oxide nanoparticles using Ceratonia siliqua and evaluation of antioxidant and cytotoxicity activities, Mater. Res. Express 6 (6) (2019) 065408.

[63] E. Nourmohammadi, H. Khoshdel-Sarkarizi, R. Nedaeinia, H.R. Sadeghnia, L. Hasanzadeh, M. Darroudi, et al., Evaluation of anticancer effects of cerium oxide nanoparticles on mouse fibrosarcoma cell line, J. Cell. Physiol. 234 (4) (2019) 4987–4996.
[64] S. Aseyd Nezhad, A. Es-haghi, M.H. Tabrizi, Green synthesis of cerium oxide nanoparticle using Origanum majorana L. leaf extract, its characterization and biological activities, Appl. Organomet. Chem. (2020;34(2):e5314.).
[65] M. Hijaz, S. Das, I. Mert, A. Gupta, Z. Al-Wahab, C. Tebbe, et al., Folic acid tagged nanoceria as a novel therapeutic agent in ovarian cancer, BMC Cancer 16 (1) (2016) 1–14.
[66] T. Alabyadh, R. Albadri, A. Es-Haghi, M.E.T. Yazdi, N. Ajalli, A. Rahdar, et al., ZnO/CeO2 nanocomposites: metal-organic framework-mediated synthesis, Characterization, and estimation of Cellular toxicity toward liver cancer cells, Journal of Functional Biomaterials. 13 (3) (2022) 139.
[67] A. Es-haghi, F. Javadi, M.E.T. Yazdi, M.S. Amiri, The expression of antioxidant genes and cytotoxicity of Biosynthesized cerium oxide Nanoparticles against hepatic Carcinoma cell line, Avicenna Journal of Medical Biochemistry. 7 (1) (2019) 16–20.
[68] M. Javad Farhangi, A. Es-haghi, M.E. Taghavizadeh Yazdi, A. Rahdar, F. Baino, MOF-mediated synthesis of CuO/CeO2 composite Nanoparticles: Characterization and estimation of the Cellular toxicity against breast cancer cell line (MCF-7), Journal of Functional Biomaterials. 12 (4) (2021) 53.
[69] S.M. Mousavi-Kouhi, A. Beyk-Khormizi, M.S. Amiri, M. Mashreghi, A. Hashemzadeh, V. Mohammadzadeh, et al., Plant gel-mediated synthesis of gold-coated nanoceria using Ferula gummosa: Characterization and estimation of its Cellular toxicity toward breast cancer cell lines, J. Functional Biomater. 14 (7) (2023) 332.
[70] V. Mohammadzadeh, M. Barani, M.S. Amiri, M.E.T. Yazdi, M. Hassanisaadi, A. Rahdar, et al., Applications of plant-based nanoparticles in nanomedicine: a review, Sustain. Chem. Pharm. 25 (2022) 100606.
[71] M.S. Amiri, V. Mohammadzadeh, M.E.T. Yazdi, M. Barani, A. Rahdar, G.Z. Kyzas, Plant-based gums and mucilages applications in pharmacology and nanomedicine: a review, Molecules 26 (6) (2021) 1770.
[72] M.E. Taghavizadeh Yazdi, A. Hamidi, M.S. Amiri, R. Kazemi Oskuee, H.A. Hosseini, A. Hashemzadeh, et al., Eco-friendly and plant-based synthesis of silver nanoparticles using Allium giganteum and investigation of its bactericidal, cytotoxicity, and photocatalytic effects, Mater. Technol. 34 (8) (2019) 490–497.
[73] M. Nadeem, R. Khan, K. Afridi, A. Nadhman, S. Ullah, S. Faisal, et al., Green synthesis of cerium oxide nanoparticles (CeO2 NPs) and their antimicrobial applications: a review, Int. J. Nanomed. (2020) 5951–5961.
[74] S.N. Naidi, M.H. Harunsani, A.L. Tan, M.M. Khan, Green-synthesized CeO2 nanoparticles for photocatalytic, antimicrobial, antioxidant and cytotoxicity activities, J. Mater. Chem. B 9 (28) (2021) 5599–5620.
[75] S. Balaji, B.K. Mandal, L. Vinod Kumar Reddy, D. Sen, Biogenic ceria nanoparticles (CeO2 NPs) for effective photocatalytic and cytotoxic activity, Bioengineering 7 (1) (2020) 26.